ISSN: 2414-1895 DOI: 10.6919/ICJE.202604_12(4).0013

Effect of Hot-Wire Arc Low-Temperature Plasma-Assisted Nitriding on the Structure and Properties of Nitrided Layers in Different Substrates

Yongqiong Ren[1,*], Wei Fang[1], Jie Chen[1], Zhihong Huang[2], Wenchang Lang[2]

[1] YongGu Group Corporation Co., Ltd., 328#20 Road, Economic Development Zone, Yueqing, Zhejiang 325600, China

[2] Wenzhou Polytechnic, Chashan Higher Education Park, Ouhai District, Wenzhou, Zhejiang 325035, China

Abstract

Hot-wire arc low-temperature plasma-assisted nitriding technology was used to perform nitriding treatment on the surfaces of AISI 430 stainless steel, AISI 304 stainless steel, and AISI M2 high-speed steel. After nitriding treatment, the phase structure of the nitrided layer of AISI 430 stainless steel is mainly composed of nitrogen-expanded ferrite phase (αN), Fe-N compounds (ε phase and γ' phase), and a small amount of CrN. The phase structure of the nitrided layer of AISI 304 stainless steel is mainly composed of nitrogen-expanded austenite phase (γN) and a small amount of CrN, while the phase structure of the nitrided layer of AISI M2 high-speed steel is mainly composed of nitrogen-expanded martensite phase (αN), Fe-N compounds (ε phase and a small amount of γ' phase), and carbide phase. After nitriding treatment, AISI 430 stainless steel has the thickest nitrided layer. The hardness of PN430 and PN304 is increased by about 700% compared with the untreated substrates, and both the friction coefficient and wear scar width are significantly reduced; while the hardness of PNGS is increased by 200% compared with the untreated substrate, and the friction coefficient and wear scar width are slightly reduced. After nitriding, the overall corrosion resistance of AISI 430 stainless steel and AISI 304 stainless steel decreases, but their pitting corrosion resistance increases, whereas both the overall corrosion resistance and pitting corrosion resistance of AISI M2 high-speed steel are improved.

Keywords

Hot-wire Arc; Low-temperature Plasma Nitriding; AISI 430; AISI 304; AISI M2; Nitrided Layer Structure.

1. Introduction

Owing to the advantages of low treatment temperature, small component deformation, high surface hardness, and excellent fatigue resistance [1] [2],surface nitriding technology has attracted increasing attention from researchers. Common nitriding methods mainly include salt bath nitriding, gas nitriding, laser nitriding, and others.However, conventional nitriding is generally carried out at 500-590 °C. It has been reported [2] that nitriding of stainless steel at such temperatures leads to the precipitation of CrN phases on the surface, reducing the content of free Cr in the substrate. The resulting Cr-depleted surface deteriorates the corrosion resistance of stainless steel.The formation of CrN is related not only to nitriding temperature but also to treatment duration; a longer holding time also promotes the precipitation of CrN. Nevertheless, low-temperature and short-time nitriding only yields a thin precipitate-free nitrided layer (usually thinner than 8 μm), which cannot provide

ISSN: 2414-1895 DOI: 10.6919/ICJE.202604_12(4).0013

sufficient load-bearing capacity even as a transition layer.This creates a contradiction: nitriding of stainless steel requires both low temperature and high nitriding efficiency, making low-temperature high-efficiency nitriding a challenging issue.

Nitriding temperature significantly influences the microstructure and properties of the nitrided layer. Sun et al. [3] found that CrN precipitation could be avoided in AISI 420 stainless steel nitrided at 400–460 °C. An ε-$Fe_{2-3}N$ layer was mainly formed on the substrate surface, which was attributed to the low diffusion rate of nitrogen at low nitriding temperatures.With increasing temperature, the nitrogen concentration and nitrided layer thickness increased slightly, possibly due to the high activity of nitrogen ions at elevated temperatures.Zhao et al. [4] further investigated the effect of nitriding temperature ranging from 380 to 580 °C on plasma-nitrided AISI 304 stainless steel.They found that at relatively high nitriding temperatures around 480 °C, the γN peaks in the XRD patterns weakened or even disappeared, accompanied by the precipitation of iron nitrides (Fe_xN, x=2-4; γ'-Fe_4N) and chromium nitrides in the nitrided layer.The formation of these nitrides was ascribed to the partial decomposition and chemical reaction of the metastable supersaturated expanded austenite phase with incoming active nitrogen during high-density plasma nitriding.Relatively stable CrN tends to form at 480 °C and above, because the high negative enthalpy and low Cr diffusivity in the substrate favor the formation of chromium nitrides at temperatures above 450 °C.In addition, they reported that at low nitriding temperatures, the improvement in microhardness mainly originated from the γN phase with compressive residual stress and micro-deformation in the high-nitrogen layer.At higher nitriding temperatures, the precipitation of iron nitrides and CrN became the dominant factor for hardness enhancement. Compared with the γN phase formed at low temperatures, iron nitrides and CrN obtained at high temperatures contributed more to hardening due to their higher hardness.

AISI 304 and AISI 430 stainless steels are widely used in kitchen appliances, medical devices, chemical containers, and automotive exhaust systems owing to their favorable corrosion resistance [5][6][7].However, the relatively low hardness and poor wear resistance of stainless steels often lead to premature failure of components caused by excessive wear.Low-temperature plasma nitriding has been proven to effectively strengthen the stainless steel surface and significantly prolong its service life.For high-speed steels, service life is also critical, and low-temperature plasma nitriding can remarkably improve their durability, thereby achieving the goals of cost reduction, efficiency improvement, and enhanced material utilization.

In this work, three typical steels were used to investigate the effects of hot-wire arc low-temperature plasma-assisted nitriding on the microstructure and properties of different substrate materials.Under identical processing parameters, the influences of hot-wire arc plasma-assisted nitriding on the structure and performance of AISI 430 stainless steel, AISI 304 stainless steel, and AISI M2 high-speed steel were experimentally studied.

2. Experimental Methods

2.1 Experimental Equipment and Materials

Nitrided samples were prepared using a self-built setup by our research group. The photograph and schematic diagram of the equipment are shown in **Figure 1**.Compared with conventional hot-wire plasma-assisted nitriding, the ionization unit of this apparatus is equipped with an auxiliary anode for attracting and accelerating electrons, in addition to an auxiliary hot wire for generating high-density electrons. The auxiliary hot wire can not only generate high-density electrons but also provide auxiliary heating. The auxiliary anode enhances the ionization of the working gas in the chamber by attracting and accelerating electrons emitted from the hot wire. Samples were suspended on a rotating rack. Through the rotation of the rack, samples were periodically and uniformly bombarded by plasma, which improves the uniformity of nitriding effects for substrates treated in the same batch.

ISSN: 2414-1895 DOI: 10.6919/ICJE.202604_12(4).0013

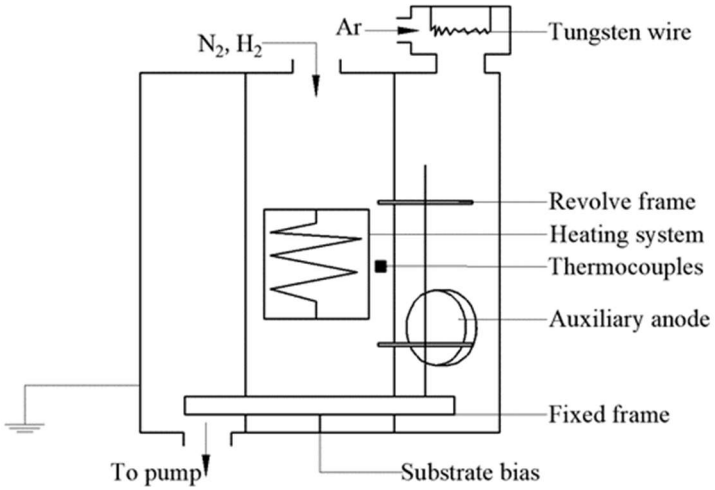

Figure 1. Hot filament arc assisted low-temperature plasma nitriding equipment

Three materials were used as substrates: AISI 430 stainless steel, AISI 304 stainless steel, and AISI M2 high-speed steel. Their chemical compositions are listed in **Table 1**.The dimensions of both AISI 430 and AISI 304 stainless steel substrates are 20 mm × 20 mm × 2 mm, while those of AISI M2 high-speed steel substrates are 16 mm × 16 mm × 4 mm. The surfaces of AISI 430 and AISI 304 stainless steel substrates are relatively smooth. AISI 430 stainless steel substrates were subjected to sandblasting to remove the surface oxide layer. In contrast, AISI M2 high-speed steel substrates possess a rough surface and thus require grinding and polishing.

Table 1. The main components of the materials used in the experiment

Name	C	Mn	P	S	Si	Cr	Ni	Cu	Mo	W	V	Fe
AISI430	0.13	0.93	0.12	0.02	0.64	17.3	/	/	/	/	/	Margin
AISI304	0.07	0.86	0.3	0.03	0.58	19.5	9.8	/	/	/	/	Margin
AISI M2	0.85	0.2	0.01	0.03	0.32	4.2	0.05	0.06	4.9	6.2	1.9	Margin

2.2 Experimental Process and Parameters

The hot-wire arc low-temperature plasma-assisted nitriding process consists of substrate pretreatment, air extraction and preheating, and nitriding. The specific procedures are as follows: (1) All samples were ultrasonically cleaned in anhydrous ethanol for 10 minutes before nitriding. After cleaning, the samples were taken out and dried with compressed air; (2) After cleaning, the samples were hung on the rotating sample rack according to experimental requirements, the vacuum chamber was closed, the vacuum degree was pumped to the background vacuum of 8.0×10^{-3} Pa, and the temperature was heated to the required experimental temperature; (3) After reaching the background vacuum, nitriding was started: the required Ar gas, N_2 gas and H_2 gas were introduced to achieve the corresponding nitrogen-hydrogen ratio and gas pressure. The filament power supply and anode power supply were turned on in sequence and set to the predetermined values, then the bias power supply was turned on and set to the predetermined value. Finally, the timer was turned on, and the time was set to 100 minutes; (4) After the experiment, the anode power supply, filament power supply and bias unit were turned off in sequence, and finally the gas filling system was turned off. After the vacuum chamber temperature dropped below 150 °C, the air extraction system was turned off, the furnace was opened to take out the samples, and the experiment was completed.

The experimental parameters are listed in **Table 2**. For the convenience of discussion, the untreated substrates and nitrided samples with different structures are denoted as UT430, UT304, UTGS, PN430, PN304, and PNGS, respectively.

ISSN: 2414-1895 DOI: 10.6919/ICJE.202604_12(4).0013

Table 2. Key parameters in the nitriding experiments of different structural substrates

Number	Partial Pressure of Working Gas (Pa)			Total Gas Pressure (Pa)	Substrate Bias (V)	Anode Current (A)	Filament Current (A)	Time (min)
	Ar	N_2	H_2					
PN430	1							
PN304		1.25	1.25	3.5	-200	80	125	100
PNGS								

2.3 Experimental Detection and Analysis

The surface of nitrided samples was observed and analyzed using a HAL100 metallographic microscope. An OLYMPUS DSX1000 digital microscope was employed to observe and measure the cross-sectional morphology and thickness of the nitrided samples. The elemental distribution along the depth was analyzed using an energy dispersive spectrometer (EDS) Xplore30 attached to a CLARA LMH field emission scanning electron microscope (FE-SEM) manufactured by TESCAN (Czech Republic). A D8 ADVANCE multi-functional X-ray diffractometer (XRD) was used to analyze the microphase structure of the nitrided samples and coated samples. For the DLC coating, its Raman spectrum was obtained using a Lab RAM HR Evolution. A HV-1000A Vickers hardness tester was used to measure the surface hardness of the nitrided samples with a load of 50 gf, and a Buehler Micromet 5103 microhardness tester was used to measure the cross-sectional hardness with a selected load of 50 g.

The wear resistance of the nitrided samples and coated samples was tested using an MS-T3000 electrostatic friction and wear tester. The friction mode was unlubricated rotational dry friction, with a 3 mm SiC ceramic ball used as the wear ball, an experimental load of 1500 g, an experimental rotation speed of 500 r/min, and an experimental time of 30 min. The polarization curves of the nitrided samples were measured using a CS350 electrochemical workstation with a three-electrode system, where the auxiliary electrode was a platinum electrode, the reference electrode was a saturated calomel electrode (SCE), and the sample was the working electrode. The electrolyte was a 3.5 wt.% NaCl solution. After the open-circuit voltage stabilized at room temperature, the anodic polarization curve test was performed at a scanning rate of 0.01 V/s.

3. Results and Discussion

3.1 Surface Morphology

Figure 2 shows the comparison of surface morphologies of substrates with different structures before and after nitriding. It can be seen that the surfaces of UT304 and UTGS are relatively smooth, while the surface of UT430 is rough with many scratches formed during sandblasting. Compared with UT430, the surface scratches of PN430 are reduced, which is attributed to the formation of nitrides and nitrogen-solid-solution expanded α-Fe phase. The formation of these phases compresses the original scratches on the untreated sample surface. In addition, the sample surface is smoothed by the bombardment of high-energy ions during nitriding.

After nitriding, great changes occur in the surface morphology. Obvious “relief” morphology appears on the surfaces of PN430 and PN304, which is a gradual transition of the characteristic surface state induced by thermochemical diffusion of nitrogen atoms. The incorporation of a high concentration of N atoms into the substrate lattice causes severe lattice distortion and high internal stress in the nitrided layer. The difference in elastic modulus among different crystal planes leads to anisotropic strain, resulting in surface relief with different degrees. Furthermore, lattice expansion caused by nitrogen dissolution is constrained in the in-plane direction, generating tensile stress in the normal direction. Such tensile stress induces lattice torsion and thus the formation of surface relief.

ISSN: 2414-1895 DOI: 10.6919/ICJE.202604_12(4).0013

PN304 exhibits the highest surface nitrogen concentration and thus the most significant relief.In contrast, the relief on PNGS is weak owing to its relatively low nitrogen concentration in the nitrided layer.Besides, the surfaces of PN430 and PNGS are uniformly covered with numerous dispersed particles and pits induced by high-energy ion bombardment.These particles are nitride precipitates formed on the sample surface when the solubility of nitrogen atoms in the substrate lattice reaches saturation during nitriding.It has been reported in Ref. [8] that these particles are mainly composed of iron nitrides, which is also confirmed by the strong iron nitride peaks in the XRD patterns of PN430 and PNGS (Figure 2).

Although the intensity of iron nitride peaks in the XRD pattern of PNGS is lower than that of PN430, denser precipitated particles are observed on its surface. It is speculated that carbide particles are also precipitated on the surface of PNGS, which is verified by the newly formed carbide peaks detected in its XRD pattern (Figure 2 (c)).

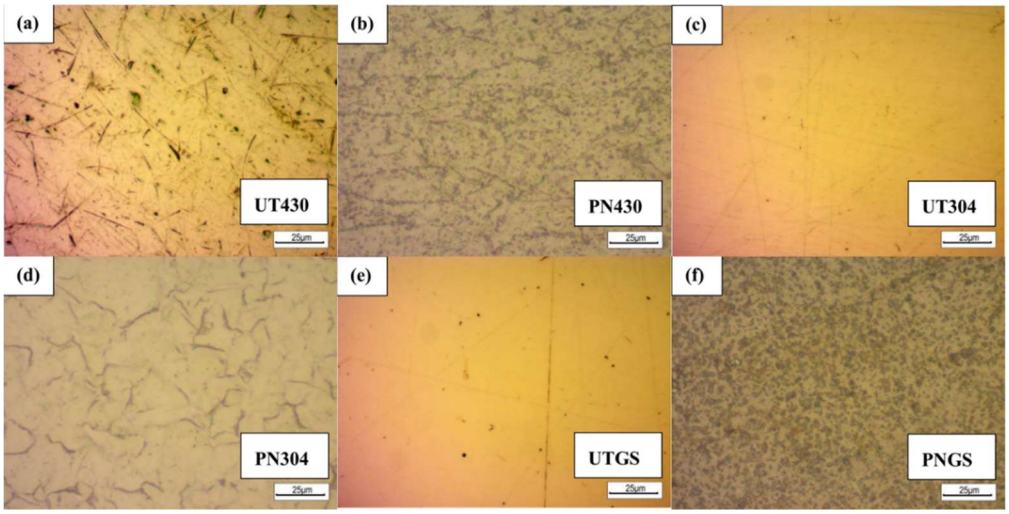

Figure 2. Comparison of surface morphologies of different material substrates before and after nitriding

3.2 Nitrided Layer Thickness and Nitrogen Concentration Distribution

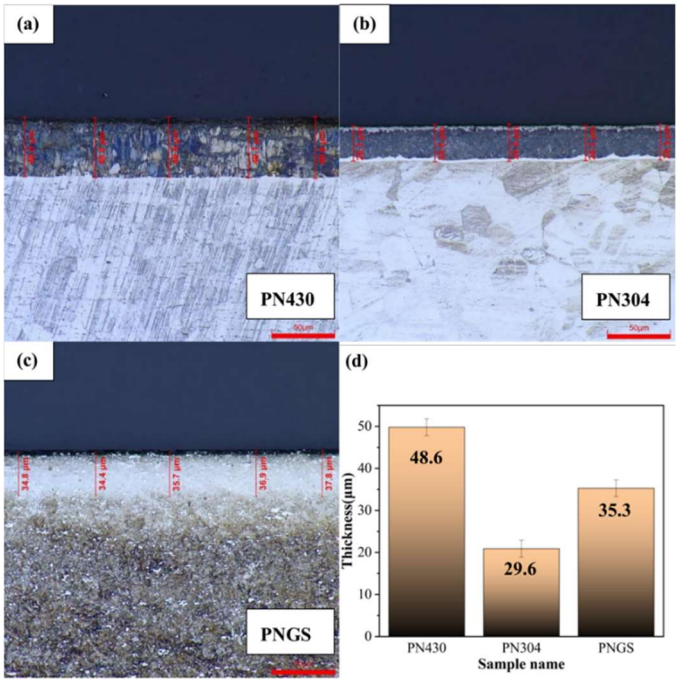

Figure 3. Comparison of cross-sectional morphologies and thickness of the nitriding layers on different substrates

ISSN: 2414-1895 DOI: 10.6919/ICJE.202604_12(4).0013

Figure 3 shows the cross-sectional morphologies and thicknesses of the nitrided layers for substrates with different structures after nitriding. Obvious boundaries exist between the nitrided layers and the grain boundaries in PN304 and PN430, which is attributed to the different crystal structures between the nitrided layers and the substrates. The interface between the nitrided layer and the substrate is relatively vague in PNGS. This is related to the low nitrogen concentration in the nitrided layer near the substrate. The low nitrogen concentration leads to a negligible microstructural change compared with the substrate, thus resulting in a blurry interface between the nitrided layer and the substrate.

Significant differences exist in the nitrided layer thickness among the three nitrided substrates.Specifically, PN430 possesses the thickest nitrided layer at 48.6 μm, followed by PNGS at 35.3 μm, and PN304 has the thinnest layer at 29.6 μm.Such differences in layer thickness are related to the distinct microstructures and chemical compositions of the three substrates.

During plasma nitriding, nitrogen atoms dissolve and diffuse into the substrate mainly via interstitial sites.Both body-centered cubic (BCC) and face-centered cubic (FCC) lattices contain tetrahedral and octahedral interstices.Since the octahedral interstices are larger than the tetrahedral ones in both structures, nitrogen atoms require less energy to occupy octahedral sites, indicating that N atoms prefer to diffuse through octahedral interstices.

In addition, it has been reported that the solvation energy of interstitial atoms in octahedral sites (5.31 eV) is higher than that in tetrahedral sites (4.53 eV), making foreign atoms more stable in octahedral interstices.Therefore, for substrates with different crystal structures, PN430 and PNGS with a BCC structure, which provides more octahedral interstices, should exhibit thicker nitrided layers, while PN304 with an FCC structure presents a thinner layer.

Furthermore, the alloying elements in the substrate also affect the nitrided layer thickness.In general, Cr has a stronger chemical affinity with N (−22 kJ·mol^{-1}) than Fe does with N (−8 kJ·mol^{-1}).Thus, a higher Cr content in the substrate hinders the diffusion of N atoms, which is one of the main reasons for the thinner nitrided layer in PN304 compared with PN430 and PNGS.

Although the Cr content in high-speed steel is lower than that in 430 stainless steel, the nitrided layer thickness of PNGS is still lower than that of PN430.By comparing the elemental compositions of high-speed steel, 430 stainless steel, and 304 stainless steel, it can be found that high-speed steel contains additional elements such as Mo, W, and V, which also exhibit high affinity with N.Moreover, these elements increase the lattice distortion of the metallic substrate, further impeding the lattice diffusion of N atoms and thus reducing the nitrided layer thickness of PNGS.

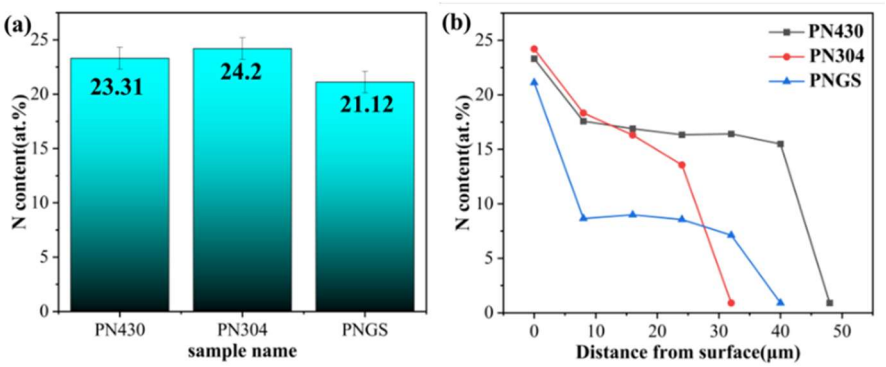

Figure 4. Surface nitrogen concentration (a) and cross-sectional nitrogen concentration distribution (b) of the nitriding layers on different substrates

Both AISI 304 and AISI 430 stainless steels possess a high Cr content. Cr atoms occupy lattice sites, and nitrogen atoms preferentially occupy octahedral interstices close to Cr lattice sites. Once trapped at these sites, N atoms can hardly escape and diffuse further into the substrate. Such interstitial sites in the octahedral positions are defined as trapping sites.

ISSN: 2414-1895 DOI: 10.6919/ICJE.202604_12(4).0013

Therefore, high nitrogen concentrations appear near the surface of the nitrided layers in PN304 and PN430, as shown in Figure 4. Since the Cr content in AISI 304 stainless steel is higher than that in AISI 430 stainless steel, N atoms are more easily trapped by Cr atoms on the sample surface, resulting in a higher surface nitrogen concentration in PN304 than in PN430. AISI M2 high-speed steel has the lowest Cr content among the three substrates, thus exhibiting the lowest surface nitrogen concentration.

The cross-sectional nitrogen concentration distributions of the nitrided layers for different substrates are displayed in the figure. All samples exhibit a three-stage distribution: the nitrogen concentration gradient is relatively large near the outermost surface and near the substrate, while it is gentle in the middle region of the nitrided layer.

The nitrogen concentration gradient in the middle of the nitrided layer of PN304 is steeper than those of PN430 and PNGS, indicating poorer diffusivity of N atoms in AISI 304 stainless steel during nitriding. This is related to its higher Cr content: a higher Cr content gives rise to more N trapping sites in octahedral interstices, and fewer available diffusion sites for N atoms to penetrate deeper into the substrate. This reduces the diffusion efficiency of nitrogen atoms toward the interior, leading to a rapid drop in nitrogen concentration in the middle region of the nitrided layer of PN304.

Although AISI M2 high-speed steel has the lowest Cr content among the three substrates, the nitrogen concentration near the surface of the PNGS nitrided layer changes drastically, as observed in the figure. This is attributed to the large amount of alloying elements with high chemical affinity to N, which further hinder the inward diffusion of nitrogen atoms.

3.3 Microstructural Phase Composition

Figure 5 shows the microstructural phase compositions of the nitrided and untreated samples. After treatment by hot-wire arc low-temperature plasma-assisted nitriding, the substrate diffraction peaks of all samples exhibited varying degrees of shift and intensity reduction, which resulted from lattice distortion caused by the dissolution of nitrogen atoms into the substrate lattice. The peak shift showed good consistency with the surface nitrogen concentration: the higher the surface nitrogen concentration, the more obvious the peak shift.

Different substrates exhibited distinct phase structures after nitriding. The phase structure of the nitrided layer in PN430 mainly consisted of nitrogen-expanded ferrite α_n, Fe-N compounds (ε phase and γ'phase), and a small amount of CrN. The nitrided layer of PN304 was mainly composed of nitrogen-expanded austenite γ_n and a small amount of CrN. In addition, a small peak appeared on the right side of the γ(111) peak of UT304, which was identified as martensite α phase formed during the manufacturing process [9].After nitriding, the width of this martensite peak increased, indicating that nitrogen atoms dissolved into the martensite lattice.

The nitrided layer of PNGS was mainly composed of nitrogen-expanded martensite α_n, Fe-N compounds (ε phase and a small amount of γ'phase), and carbides. No CrN was detected in PNGS.

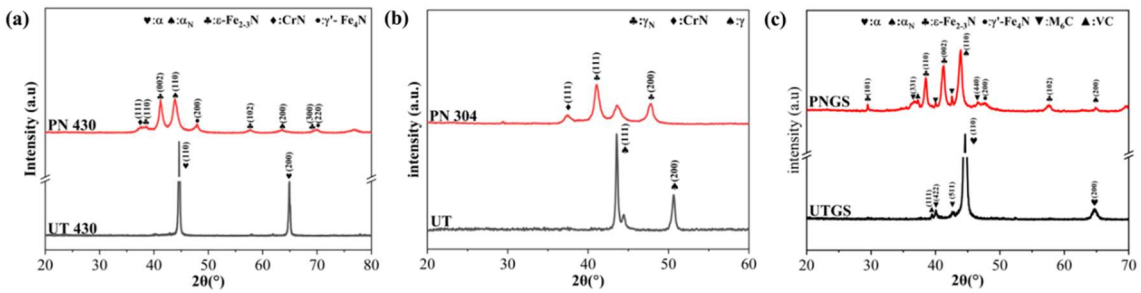

Figure 5. X-ray diffraction patterns of the nitriding layers on different substrates

Compared with UT304, only nitrogen-expanded austenite γ_n and CrN phases appeared in PN304, while other nitrides such as Fe-N compounds were not formed.In contrast, besides nitrogen-expanded

ISSN: 2414-1895 DOI: 10.6919/ICJE.202604_12(4).0013

ferrite α_n and CrN, Fe-N compounds (ε phase and γ' phase) were also observed in PN430.This phenomenon is presumed to be related to the higher carbon content in AISI 430 stainless steel than in AISI 304 stainless steel (Table).It has been reported in the literature that a relatively high carbon content contributes to the formation and stabilization of the ε-$Fe_{2-3}N$ phase [10].The formation of γ'-Fe_4N is speculated to be related to the relatively high surface temperature of the cathode sample induced by high-energy ion bombardment during nitriding.

Generally, a low nitrogen concentration and a relatively high temperature during nitriding can promote the formation of γ'-Fe_4N.Nevertheless, the nitrided layer of PNGS is still dominated by ε-$Fe_{2-3}N$.By comparing the chemical compositions of AISI 430 stainless steel and high-speed steel, it can be seen that high-speed steel has a higher carbon content, which facilitates the formation and stabilization of ε-$Fe_{2-3}N$.It is worth noting that, compared with UTGS, PNGS not only exhibits nitride peaks but also shows enhanced original carbide peaks and several newly formed carbide peaks.This is attributed to the high temperature during nitriding, which promotes the reaction between free carbon and metallic elements in high-speed steel to form carbides.In fact, elements such as V, Cr, W, and Mo can react with C to form simple carbides (e.g., VC) and complex carbides such as $(Fe,Cr)_3(W,Mo)_3C$ [11].

3.4 Surface and Cross-Sectional Hardness

The surface hardness of the three different substrates after nitriding is shown in Figure 6 (a).The hardness of PN430 after nitriding is 1556.6 $HV_{0.05}$, which is approximately 700% higher than that of UT430 (196.5 $HV_{0.05}$).PN304 exhibits a lower hardness of 1474.2 $HV_{0.05}$ compared with PN430, representing an increase of about 700% relative to UT304 (212.2 $HV_{0.05}$).

The improvement in surface hardness for PNGS is less significant than those for PN430 and PN304.The hardness increases merely from 653.8 $HV_{0.05}$ for UTGS to 1226.6 $HV_{0.05}$ for PNGS, with an increment of only about 200%.

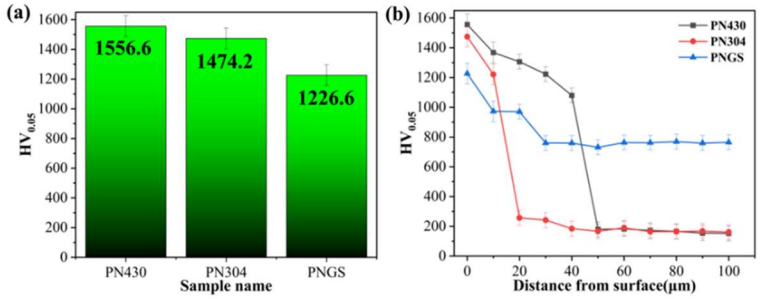

Figure 6. Surface nitrogen concentration (a) and cross-sectional nitrogen concentration (b) of different nitriding substrates

The significant increase in hardness after nitriding is mainly attributed to three factors:(1)Nitrogen atoms dissolve into the substrate lattice during nitriding, causing lattice distortion and thereby inducing solid-solution strengthening; (2)Metallic atoms in the substrate react with nitrogen atoms to form nitrides, which result in dispersion strengthening and hinder the nucleation and movement of dislocations; (3)A large compressive stress is generated inside the substrate after nitriding, which resists plastic deformation.

The difference in hardness among various nitrided substrates is related to their distinct nitrogen concentrations and phase structures.By comparing the shift and intensity of the substrate peaks of PN430 and PN304 in Figure 5, it can be found that the solubility of N atoms in the lattice of PN430 is lower than that in PN304, leading to slightly weaker solid-solution strengthening and compressive stress.However, abundant nitride phases (such as Fe-N compounds (ε phase and γ'phase) and CrN) are detected in the nitrided layer of PN430.These nitrides provide considerable dispersion strengthening, which compensates for the disadvantages caused by the relatively low surface nitrogen

ISSN: 2414-1895 DOI: 10.6919/ICJE.202604_12(4).0013

concentration and weak solid-solution effect.In addition, PN430 possesses a thicker nitrided layer than PN304, so the surface hardness of PN430 is slightly higher than that of PN304.For PNGS, owing to its low surface nitrogen concentration, the content of formed nitride phases is lower than that in PN430.Thus, the solid-solution strengthening, dispersion strengthening, and compressive stress induced by nitriding are all relatively weak, resulting in the lowest surface hardness.

Figure 6 (b) illustrates the cross-sectional hardness distribution of the nitrided layers for different substrates.The cross-sectional hardness is in good agreement with the cross-sectional nitrogen concentration.PN430 shows the highest cross-sectional nitrogen concentration, which brings greater solid-solution strengthening and compressive stress, thus leading to higher cross-sectional hardness.

Although PN304 exhibits a slightly higher cross-sectional nitrogen concentration than PN430 within 14 μm from the surface, its nitrided layer is thinner, and the nitrogen concentration is lower beyond 14 μm.Consequently, its cross-sectional hardness is lower than that of PN430.PNGS presents the lowest cross-sectional hardness due to its lowest cross-sectional nitrogen concentration.

3.5 Friction and Wear Properties

Figure 7 (a-c) shows the comparison of friction coefficients of different substrates before and after nitriding.As can be seen, the wear resistance of all substrates is improved after nitriding, and the friction coefficient rises more slowly at the initial running-in stage.The friction coefficient of PN430 becomes stable at about 20 min, while those of PN304 and PNGS reach stability at approximately 4 min and 5 min, respectively.This phenomenon is attributed to the prolonged running-in period caused by the increased surface hardness.

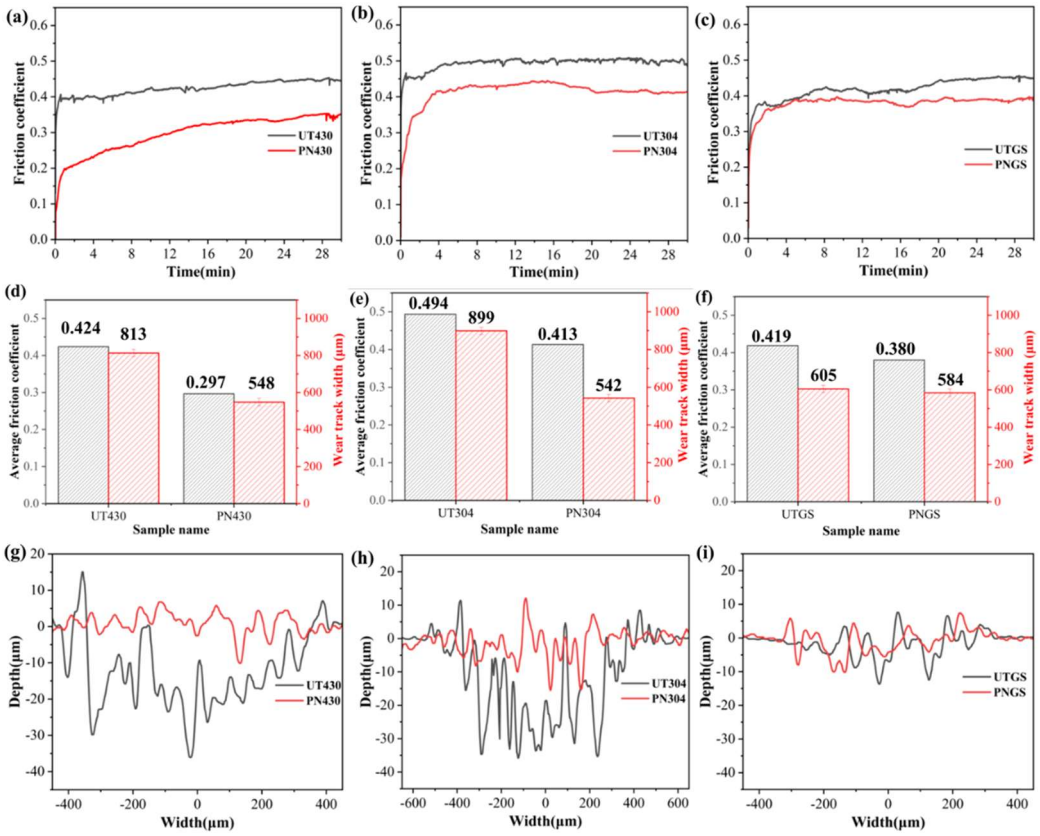

Figure 7. Variation of friction coefficient with time for different nitriding substrates (a~c), comparison of average friction coefficient and wear track width (d~f), and comparison of wear track depth (g~i)

Figure 7 (d-i) displays the comparisons of the average friction coefficient, wear track width, and wear track depth of different substrates before and after nitriding.Owing to the high hardness and high

ISSN: 2414-1895 DOI: 10.6919/ICJE.202604_12(4).0013

supersaturated nitrogen concentration in the nitrided layer, the average friction coefficient, wear track width, and wear track depth of all samples are significantly reduced after nitriding, indicating that nitriding treatment can remarkably improve the wear resistance of the substrates.

3.6 Friction and Wear Properties

Figure 8 shows the wear track morphologies of different substrates before and after nitriding.As shown in the figure, UT430 and UT304 exhibit similar characteristics: the interior of the wear tracks appears dark black.Upon further magnification (Figure 8 (a) and Figure 8 (g)), obvious ploughing grooves can be observed inside the wear tracks, accompanied by a large amount of black wear debris adhered to the surface.In addition, the wear tracks of UT430 and UT304 are very rough with severe plastic deformation.

In contrast to UT430 and UT304, the wear track surface of UTGS is light-colored.After magnification (Figure 8 (h)), colored oxide films are found on the surface, indicating the occurrence of oxidative wear.Meanwhile, the ploughing grooves inside the wear track are relatively shallow, which is attributed to the higher hardness of UTGS compared with UT430 and UT304.In summary, the wear mechanisms of UT430 and UT304 are dominated by adhesive wear and severe abrasive wear, while UTGS is dominated by oxidative wear and mild abrasive wear.

After nitriding, the surface hardness is significantly improved.The wear tracks of PN430 and PN304 become lighter, the brown wear debris disappears, and colored oxides appear on the surface, making the wear track much smoother.The wear track morphology of PNGS is similar to that of UTGS, owing to the relatively small increment in hardness compared with PN430 and PN304.

Ploughing grooves exist on the wear track surfaces of all nitrided samples, which are caused by the spalling of hard nitride particles during friction and wear.Compared with the untreated samples, both the number and depth of grooves in PN304 and PN430 are greatly reduced, indicating that the wear resistance of AISI 304 and AISI 430 stainless steels is significantly improved after nitriding.

Compared with PN430, PN304 exhibits a much larger number of ploughing grooves.On the one hand, the hardness of the nitrided layer of PN304 is relatively low.On the other hand, PN304 possesses the highest nitrogen solubility in the nitrided layer, resulting in high internal stress, which makes the nitrided layer prone to brittle spalling during wear and thus aggravates abrasive wear.

For PNGS, since the increase in hardness is less significant than that of PN430 and PN304, the number and depth of ploughing grooves show little change.Moreover, due to its lowest nitrided layer hardness, PNGS exhibits more and deeper grooves than PN304 and PN430.

In summary, the wear mechanisms of PN430, PN304, and PNGS are all dominated by oxidative wear and relatively mild abrasive wear.

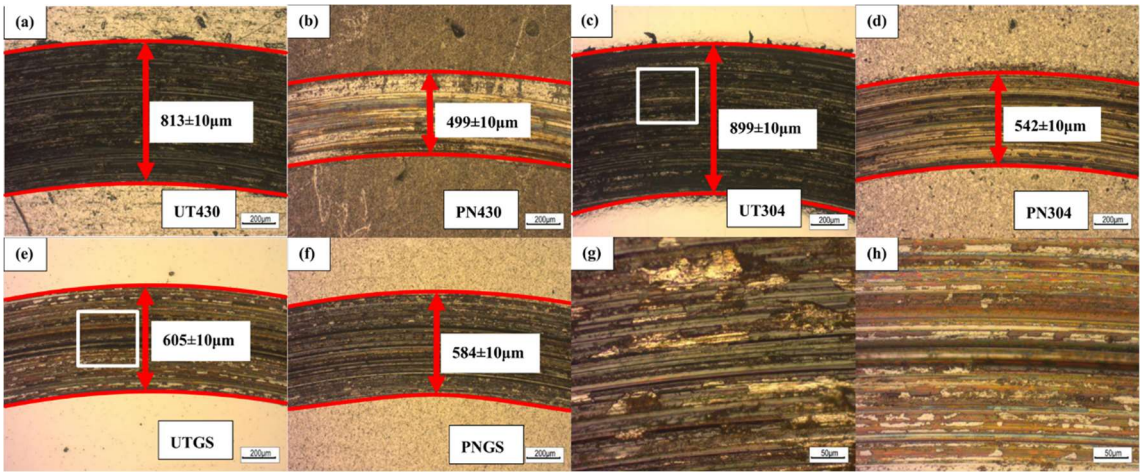

Figure 8. Comparison of wear track morphologies of different nitriding substrates(g~h) Local magnified views of UT304 and UTGS

ISSN: 2414-1895 DOI: 10.6919/ICJE.202604_12(4).0013

3.7 Corrosion Resistance

Figure 9 shows the polarization curves of the nitrided layers formed on different substrates after nitriding.Figure 10 presents the surface morphology comparison of different substrates before and after polarization. Table 3 lists the corrosion potential Ecorr and corrosion current density I corr obtained from the polarization curves.

According to Table 3, UT304 stainless steel exhibits the best corrosion resistance, followed by UT430, and UTGS shows the poorest corrosion resistance.This difference is related to the distinct Cr contents in these substrates.During electrochemical measurements, Cr atoms react with oxygen molecules in the electrolyte to form a passive film mainly composed of chromium oxide (Cr_2O_3).This passive film can effectively isolate the metallic substrate from the corrosive solution and prevent further corrosion.Therefore, substrates with different Cr contents possess different corrosion resistances.

The number of corrosion pits in Figure 10 (a) and (c) confirms this trend: UT304 has the fewest corrosion pits, while UTGS has the most.In addition, the surface of UTGS turns dark after electrochemical corrosion, suggesting that general corrosion occurs on the surface of UTGS during the test.

After nitriding, a large number of CrN precipitates form in the nitrided layers of PN430 and PN304, which reduces the concentration of free Cr atoms in the lattice.Consequently, the ability to form a protective passive film on the sample surface during electrochemical corrosion is weakened.Thus, the overall corrosion resistance of PN430 and PN304 decreases significantly compared with the untreated substrates.

The degradation in corrosion resistance is more severe for PN430 than for PN304.No passivation region is observed in the polarization curve of PN430, whereas a distinct passivation region appears for PN304 in the potential range of −0.0533 V to 0.158 V.This is because the Cr content of 430 stainless steel is lower than that of 304 stainless steel (Table 1).Although CrN is formed in both PN430 and PN304, the number of free Cr atoms remaining in the lattice of PN304 is still higher than that in PN430, leading to better overall corrosion resistance of PN304.

However, due to the higher nitrogen concentration in the nitrided layer of PN430, the size of corrosion pits on PN430 after polarization is smaller than that on PN304.

Although neither UTGS nor PNGS shows an obvious passivation region due to their low Cr contents, PNGS exhibits better corrosion resistance than UTGS (Table 3).This can be attributed to the complex chemical composition of high-speed steel, which possesses higher configurational entropy and a more distorted lattice than 304 and 430 stainless steels.After nitriding, the diffusion of nitrogen atoms further increases lattice distortion.

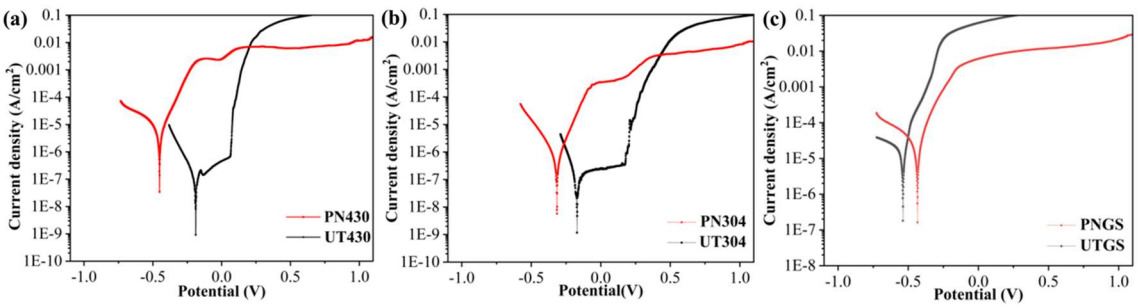

Figure 9. Comparison of anodic polarization curves of different nitriding substrates

As shown in Figure 11, after electrochemical corrosion, the size and number of corrosion pits on all nitrided samples are significantly reduced, indicating that the nitrided samples possess better pitting corrosion resistance.In addition, compared with the untreated substrate after corrosion, PN430 not only shows changes in the number and size of corrosion pits but also exhibits a darker surface color. It is speculated that general corrosion occurs on the surfaces of PN430 and PN304 after

ISSN: 2414-1895 DOI: 10.6919/ICJE.202604_12(4).0013

electrochemical corrosion, which is related to the decreased corrosion resistance caused by the reduction of free Cr atoms in the lattice.Since PN304 has a relatively higher concentration of free Cr atoms than PN430, its corrosion resistance is higher, and no obvious color change is observed on its surface after electrochemical corrosion.After electrochemical corrosion, the surface color of PNGS is lighter than that of the untreated UTGS, indicating that the degree of general corrosion is weakened. This proves that nitriding treatment significantly improves the corrosion resistance of PNGS.

Table 3. Fitting results of polarization curves for different structural substrates before and after nitriding

Sample name	Ecorr, V (vs. SCE)	I_p, A/cm^2
UT430	−0.1747	8.88×10^{-8}
UT304	−0.1576	7.69×10^{-8}
UTGS	−0.5707	2.25×10^{-5}
PN430	−0.4402	5.99×10^{-6}
PN304	−0.3127	5.55×10^{-7}
PNGS	−0.436	1.99×10^{-5}

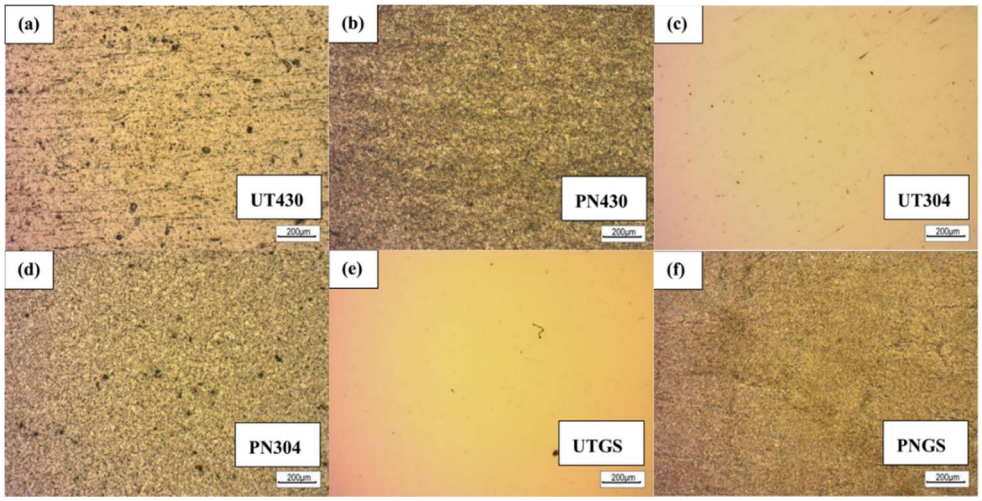

Figure 10. Surface morphologies of different substrate before polarization

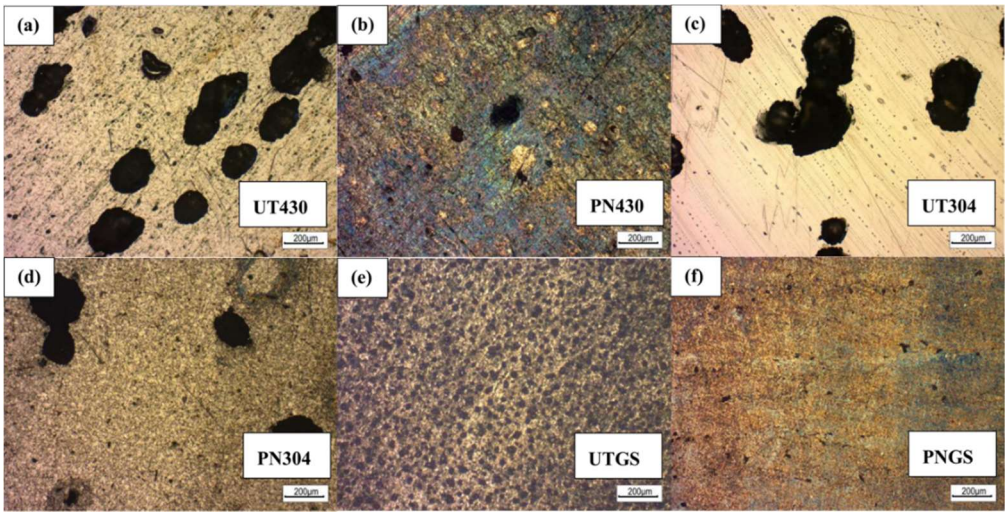

Figure 11. Surface morphologies of different substrates after polarization

ISSN: 2414-1895 DOI: 10.6919/ICJE.202604_12(4).0013

4. Conclusion

In this work, AISI 430 stainless steel, AISI 304 stainless steel, and high-speed steel were nitrided via hot-wire arc low-temperature plasma-assisted nitriding. The main conclusions are drawn as follows:

(1) Nitriding treatment can effectively remove scratches on the substrate surface. A “relief” structure appears on the surface of some nitrided samples, and the relief becomes more significant with increasing surface nitrogen concentration.

(2) The nitrided layer thickness and cross-sectional nitrogen concentration distribution of different nitrided samples are greatly affected by the substrate structure and alloying elements. PN430, with a body-centered cubic (BCC) structure and fewer elements with high nitrogen affinity, possesses the thickest nitrided layer.

(3) Different substrates exhibit distinct phase structures after nitriding:The nitrided layer of PN430 mainly consists of nitrogen-expanded ferrite α_n, Fe-N compounds (ε phase and γ’phase), and a small amount of CrN.The nitrided layer of PN304 is mainly composed of nitrogen-expanded austenite γ_n and a small amount of CrN.The nitrided layer of PNGS mainly contains nitrogen-expanded martensite α_n, Fe-N compounds (ε phase and minor γ’phase), and carbides.

(4) Nitriding improves the hardness and wear resistance of substrates with different degrees.The hardness reaches 1556.6 $HV_{0.05}$ for AISI 430 stainless steel, 1474.2 $HV_{0.05}$ for AISI 304 stainless steel, and 1226.6 $HV_{0.05}$ for AISI M2 high-speed steel.After nitriding, the friction coefficient, wear track width, and depth of all samples decrease, indicating enhanced wear resistance.The wear mechanism of AISI 430 and AISI 304 stainless steels changes from adhesive wear and abrasive wear to oxidative wear and mild abrasive wear, while that of AISI M2 high-speed steel shows no obvious variation, i.e., oxidative wear and abrasive wear.

(5) After nitriding, the corrosion resistance shows different trends:The general corrosion resistance of PN430 and PN304 decreases, while their pitting corrosion resistance is improved.For PNGS, both the general corrosion resistance and pitting corrosion resistance are enhanced.

References

[1] Gredelj S, Gerson A, Kumar S,et al. Inductively coupled plasma nitriding of aluminium[J]. Applied Surface Science, 2002, 199(1-4):183-194.

[2] ZhenGuo H, Zixin L, Lei G,et al. Structure and corrosion behavior of ultra-thick nitrided layer produced by plasma nitriding of austenitic stainless steel[J]. Surface & Coatings Technology, 2021, 405(1):126689.

[3] Ji Sun, Jie Li, J.M. Xie, Yang Yang,et al. Properties of rapid arc discharge plasma nitriding of AISI 420 martensitic stainless: effect of nitriding temperatures[J]. Journal of Materials Research and Technology, 2022,19:4804-4814.

[4] Zhao Y , Yu B , Dong L ,et al. Low-pressure arc plasma-assisted nitriding of AISI 304 stainless steel[J].Surface & Coatings Technology, 2012, 210(none):90-96.

[5] Sun B ,Liu S ,Xiao C , et al.Insights into the effect of plasma nitriding on corrosion behavior of 304 stainless steel in liquid lead-bismuth eutectic[J].Materials Chemistry and Physics,2025,339:130790-130790.

[6] Shen H ,Wang L ,Sun J .Characteristics and properties of CrN compound layer produced by plasma nitriding of Cr-electroplated of AISI 304 stainless steel[J].Surface & Coatings Technology,2020,385:125450-125450.

[7] Kochmański P ,Bielawski J ,Baranowska J .Effect of low temperature gas nitriding on corrosion properties of duplex stainless steel[J].Surface & Coatings Technology,2025,517:132842-132842.

[8] Aydin H , Bayram A , et al. Friction Characteristics of Nitrided Layers on AISI 430 Ferritic Stainless Steel Obtained by Various Nitriding Processes[J]. Materials Science-medziagotyra, 2013, 19(1):19-24.

[9] Yang L, Shangzhou Z, Yongong H, et al. Characteristics of the nitrided layer formed on AISI 304 austenitic stainless steel by high temperature nitriding assisted hollow cathode discharge[J]. Materials and Design, 2014, 64: 527-534.

ISSN: 2414-1895 DOI: 10.6919/ICJE.202604_12(4).0013

[10] Mohammadzadeh R , Akbari A , Drouet M .Microstructure and wear properties of AISI M2 tool steel on RF plasma nitriding at different N2–H2 gas compositions[J].Surface & Coatings Technology, 2014, 258:566-573.

[11] Akbari A , Mohammadzadeh R , Templier C ,et al. Effect of the initial microstructure on the plasma nitriding behavior of AISI M2 high speed steel[J]. Surface and Coatings Technology, 2010, 204(24):4114-4120.